Intermolecular correlations in an ionic liquid under shear

Intermolecular correlations in an ionic liquid under shear

S G Raju and S Balasubramanian[1]

Chemistry and Physics of Materials Unit, Jawaharlal Nehru Centre for Advanced Scientific Research, Jakkur, Bangalore 560 064, India

E-mail: raju@jncasr.ac.in and bala@jncasr.ac.in

Abstract
The behavior of a model room temperature ionic liquid under shear is explored using non-equilibrium molecular dynamics simulations. The external field reduces intermolecular structure in the liquid. However, orientational ordering of the molecules in the form of a nematic phase is observed under shear.

(Some figures in this article are in colour only in the electronic version)

1. Introduction

Room temperature ionic liquids (ILs) based on the imidazolium cation are fascinating compounds that exhibit interesting phase behavior [1–6]. The microscopic origin of the variety in phases is the competition between Coulombic and dispersive interactions [7]. The former contributes to the ordering between the cation's head group and the anion, while the latter manifests itself in alkyl tail–tail interactions. The interplay of these forces leads, for example, to structural order in the nanoscale regime in an otherwise homogeneous liquid. This nanoscale ordering has been demonstrated through computer simulations [8–12] and also by small-angle x-ray scattering experiments [13, 14].

The effect of shear on atomic and molecular liquids has been investigated by molecular dynamics simulations earlier [15, 16]. Apart from orientational ordering in a direction parallel to the shear, such studies have also shown hexagonal in-plane ordering, particularly in simple, atomic fluids. Whether room temperature ionic liquids too exhibit such a behavior is yet unknown. There have been reports of the formation of liquid crystalline phases in ILs under the application of shear [17]. Here, we report molecular dynamics simulations of an IL with a medium length alkyl tail subjected to planar Couette shear flow. Anticipating our results, we find evidence for nematic ordering of the molecular ions and significant changes in the intermolecular structure.

[1] Author to whom any correspondence should be addressed.

2. Details of simulation

A coarse-grained (CG) model was used to simulate liquid $[C_{10}mim][PF_6]$. We provide here a brief description of the model which is illustrated in figure 1. Details can be found in [11]. The cation in $[C_{10}mim][PF_6]$ contains 43 atoms. The coarse-grained representation of the cation, in turn, contains 6 beads. The imidazolium ring, along with the methyl and methylene groups bonded to the nitrogen atom, constitute three beads, while the alkyl tail is represented by three beads, CM, CM and CT. The former three beads are charged, while the latter three are neutral. Neighboring beads in the cation are connected by a harmonic spring, and a pair of beads separated by two bonds interact via a harmonic angle bending term as well. The parameters for these interactions are calculated by fitting the probability distribution of pair distances and angles obtained from an atomistic MD simulation. The anion (PF_6), being spherical, is easily represented by one bead. The potential of interaction between the CG beads contains Coulombic (charge–charge) as well as a soft dispersive term (the 9–6 interaction). The CG model has been validated against experimental results and atomistic simulations earlier [11].

The simulated system consisted of 3375 ion pairs with a total of 23 625 beads (super-atoms). Our earlier work on equilibrium simulations of ionic liquids using the CG model vividly brought out the nanoscale ordering in them [11]. The ordering is due to microphase segregation of polar and non-polar moieties. The starting configurations for the current simulation non-equilibrium simulations were obtained from our earlier study. Prior to the MD runs under shear, the system was equilibrated under constant *NVT* conditions for 400 ps.
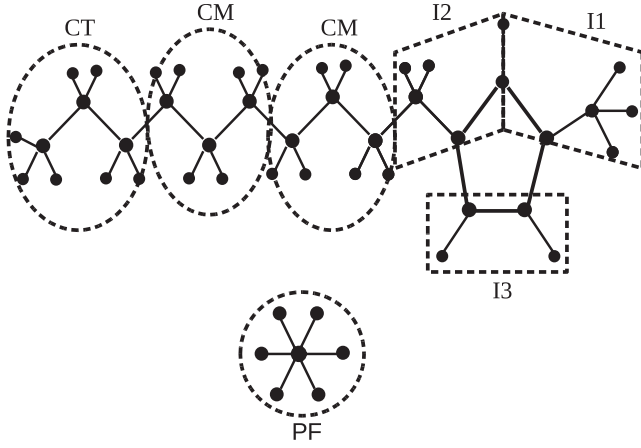
Figure 1. Schematic of [C$_{10}$mim][PF$_6$], illustrating the mapping between atoms and coarse-grained beads.

Figure 2. Isotropically averaged, neutron-weighted structure factor of liquid [C$_{10}$mim][PF$_6$] subjected to shear flow at different rates. Legends are rates in units of fs^{-1}.

The equilibrated liquid was subjected to a shear stress in the planar Couette geometry. The linear velocity flow was in the x direction and the velocity gradient was in the y direction. The SLLOD [18] equations of motion as implemented in the LAMMPS code [19] were integrated with a time step of 4 fs. The simulations were carried out at 300 K. Temperature control was achieved using Nosé–Hoover thermostats [20] with a time constant of 200 fs. Three-dimensional periodic boundary conditions consistent with the flow geometry were applied. The system was studied under four different shear rates, 0.000 01, 0.000 05, 0.0001 and 0.001 (all in units of fs^{-1}). Here, we report results at equilibrium and at the highest two shear rates. A trajectory of duration 400 ps was generated in each of these runs. The coordinates of all the beads were stored every 400 fs and were analyzed later. Typically, the initial 50 ps of the trajectory was discarded to allow the system to reach a steady state.

Coulombic interactions were treated using the particle–particle particle–mesh Ewald method with an accuracy of 10^{-6}. Pair correlation functions, $g(r)$, between distinct pairs of beads were obtained, from which the isotropic structure factor, $S(q)$, was calculated using the following relations.

The isotropically averaged partial structure factor between a pair of atom types α and β is given by

$$S_{\alpha\beta}(q) = \delta_{\alpha\beta} + 4\pi\sqrt{\rho_\alpha\rho_\beta}\int_0^\infty r^2[g_{\alpha\beta}-1]\frac{\sin(qr)}{(qr)}\,\mathrm{d}r \quad (1)$$

where $\rho_\alpha = \frac{N_\alpha}{V}$. N_α is the number of beads of type α and V is the volume of the system. The upper limit in the integral was replaced with half the box length. The isotropic total x-ray structure factor is defined as

$$S(q) = \sum_\alpha\sum_\beta c_\alpha c_\beta\frac{f_\alpha(q)f_\beta(q)}{\langle f(q)\rangle^2}S_{\alpha\beta}(q) \quad (2)$$

where c_α is the concentration of bead type α in the system. f_α is the form factor (or scattering length) of bead α and $\langle f(q)\rangle = \sum_\alpha c_\alpha f_\alpha(q)$.

In view of the presence of the symmetry breaking external field (shear), the structure factor was also calculated at each
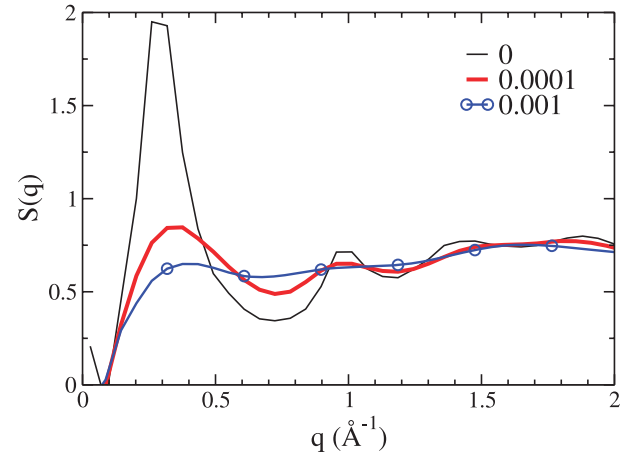
of the reciprocal space vectors, **q**. The total scattering factor, $F_T(\mathbf{q})$, is defined as [21]

$$F_T(\mathbf{q}) = \sum_{j=1}^N a_j(\mathbf{q})e^{\mathbf{i}\mathbf{q}\cdot\mathbf{r}_j} \quad (3)$$

and the scattering intensity is

$$I_T(\mathbf{q}) = F_T(\mathbf{q})F_T^*(\mathbf{q}) \quad (4)$$

where a_j is the atomic form factor of the jth species and N is the total number of atoms.

The intramolecular contribution to the scattering function and the corresponding intensity are

$$F_s^m(\mathbf{q}) = \sum_{j=1}^{N^m} a_j(\mathbf{q})e^{\mathbf{i}\mathbf{q}\cdot\mathbf{r}_j} \quad (5)$$

$$I_s(\mathbf{q}) = F_s^m(\mathbf{q})F_s^{m*}(\mathbf{q}) \quad (6)$$

where N^m is the total number of molecules. The intermolecular contribution to the scattered intensity, which provides an idea of molecular ordering, is given by

$$I_i(\mathbf{q}) = I_T(\mathbf{q}) - I_s(\mathbf{q}). \quad (7)$$

This scattering intensity ($I_i(\mathbf{q})$) was analyzed using contour plots in the three different Cartesian planes.
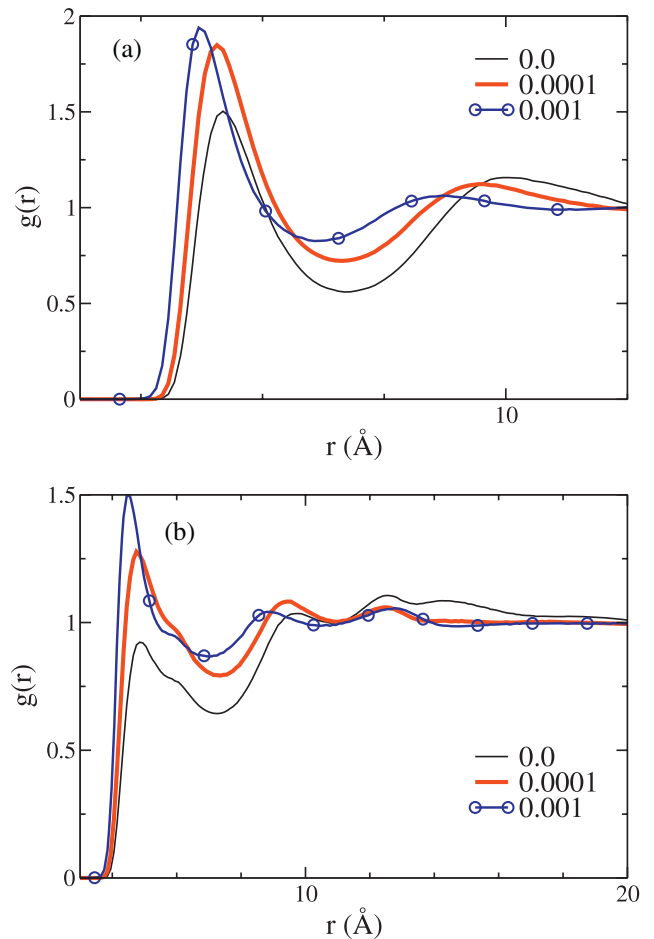
3. Results and discussion

Figure 2 compares the isotropically averaged, neutron-weighted structure factor at three shear rates: zero, 0.0001 and 0.001 fs^{-1}. The low wavevector peak at 0.3 Å^{-1} signifies intermediate range order of a length scale around 21 Å. This corresponds to roughly twice the length of the cation. Thus, the liquid at equilibrium consists of polar regions rich in cationic heads and anions, while the alkyl tail of the cation constitutes the non-polar part. The low angle peak prominently present at
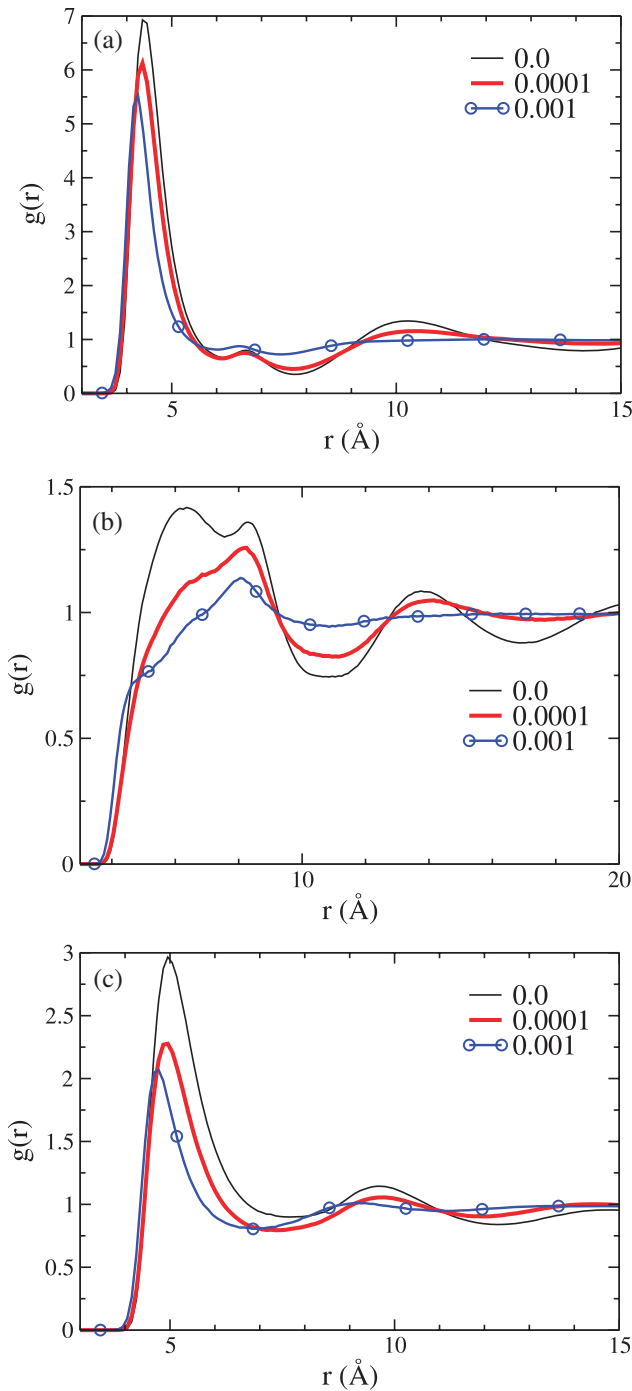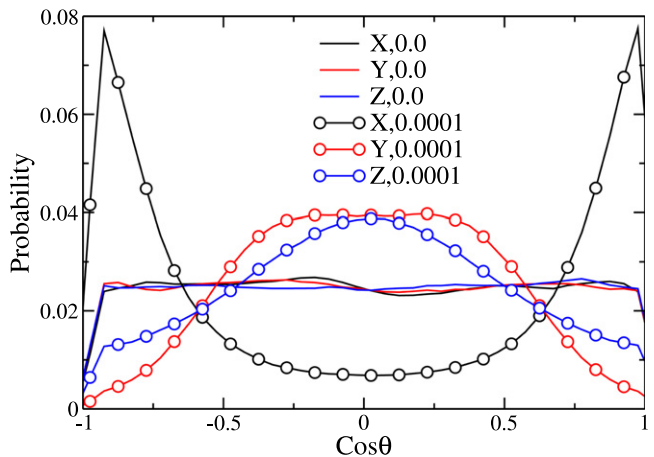
Figure 3. Partial pair correlation functions. (a) Cation's head group—anion, (b) cation's head group—head group, (c) cation's tail bead—tail bead.


Figure 4. Partial pair correlation functions. (a) Cation's tail–anion, (b) cation's head group–tail bead.

Figure 5. Probability distributions of the angle θ made by the cation's head group–tail vector with respect to the Cartesian axes. Numerical values in the legend are shear rates in units of fs^{-1}.

equilibrium decreases in intensity with increasing shear rate. Thus, shear reduces the nanoscale ordering that is intrinsically present in the ionic liquid at equilibrium. Apart from a reduced intensity, the low angle peak also shifts marginally to higher wavevectors, implying the decrease in the length scale of the nanoscale ordering.

Our earlier work showed that the 0.3 Å^{-1} peak in the total structure factor had substantial contributions from partial structure factors of tail–tail, head–head and anion–anion pairs.

It is thus important that we examine these pair correlation functions. In figure 3, we show the head–anion, head–head and tail–tail $g(r)$s at equilibrium and under shear. The head group of the cation is denoted here by the I1 bead (see figure 1 for definitions of the beads) and the tail by the CT bead. The
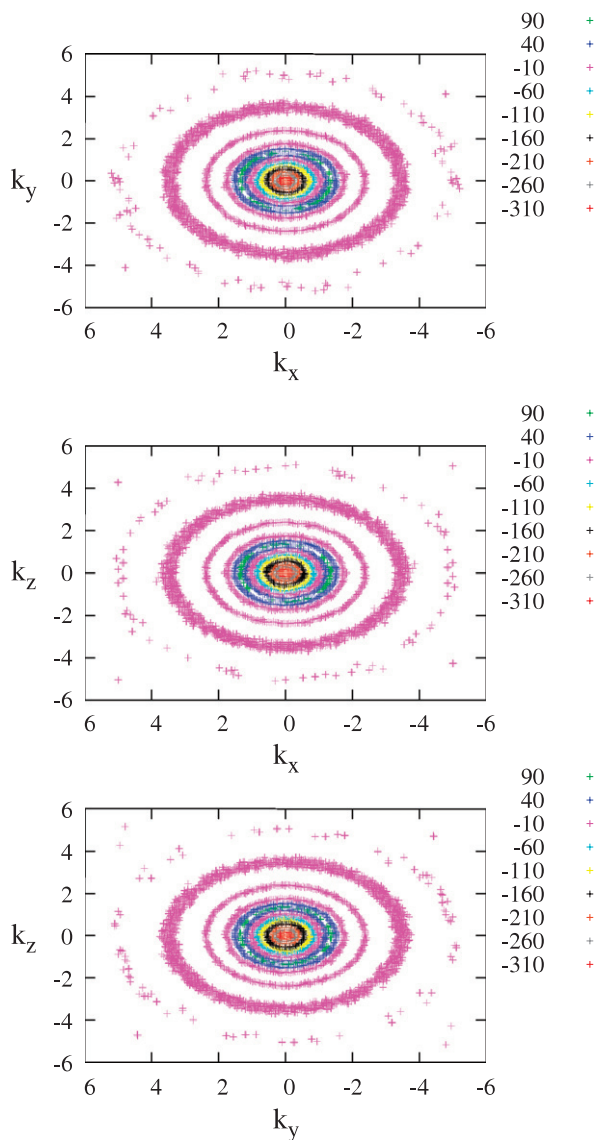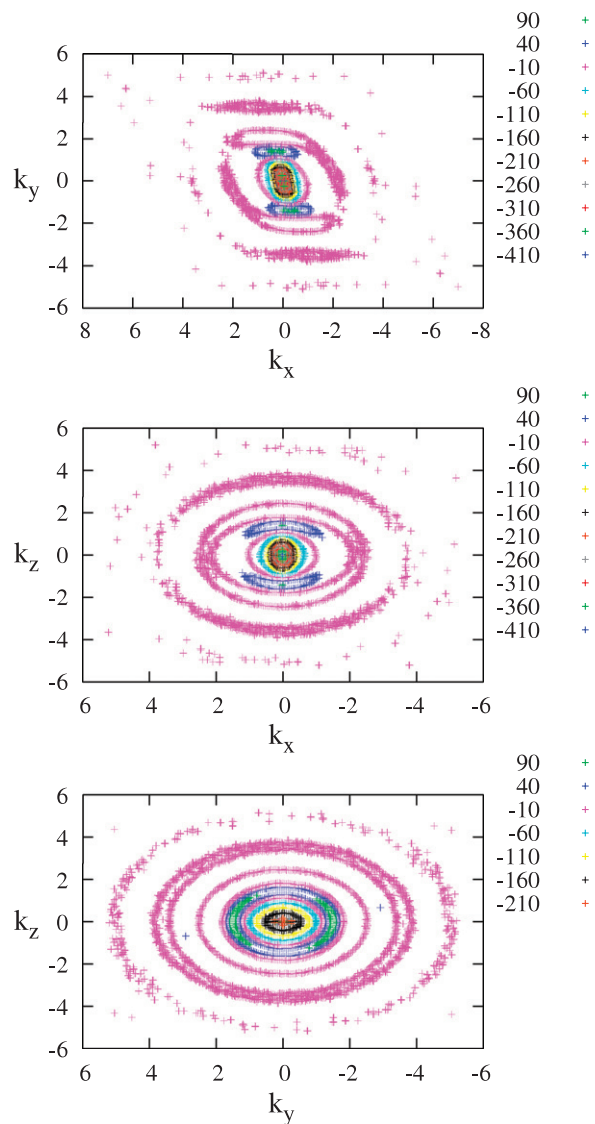
Figure 6. Contour plots of the contribution to the scattering intensity from intermolecular correlations (see equation (7)) in the ionic liquid at equilibrium, along the three distinct reciprocal lattice planes.

Figure 7. Contour plots of the contribution to the scattering intensity from intermolecular correlations (see equation (7)) in the ionic liquid at a shear rate of 0.001 fs^{-1}, along the three distinct reciprocal lattice planes.

first peak in these three functions moves to smaller distances and its intensity is reduced at high shear rates. The picture that emerges is that the liquid gets less structured under shear. Also, the distinctions between different sites (for instance, charged versus uncharged) are reduced in the presence of the external field.

In contrast to this generic behavior, two pair correlation functions exhibit an increase in the intensity of the first peak with increasing shear rate. These are for tail–anion and head–tail pairs and are shown in figure 4. The first peak in $g(r)$ for both these pairs shifts to lower distances and increases in height with increasing shear rate. Combined with the earlier observation in figure 2 of a decrease in nanoscopic order, this data implies that anions no longer have to preferentially coordinate the cation heads; they can also be present near the tails of the cation.

The externally imposed shear field can be expected to induce orientational ordering in the system. In figure 5 we

show the probability distribution of the angle that the head to tail vector of the cation makes with the three Cartesian axes. Even at a shear rate of 0.0001 fs^{-1}, the preference for cation ordering along the x axis is discernible. At the highest shear rate, this preference dominates. One finds clear evidence for the long axis of the cation to be parallel to the shear direction. Note that there is equal preference for the cation head to be along the positive and the negative x axis.

Are the cations layered along the x axis? Evidence for the absence of layering at 300 K comes from calculations of the q-dependent scattered intensity, $I_i(\mathbf{q})$, defined in equation (7). In figures 6 and 7, we show contour plots of $I_i(\mathbf{q})$ at equilibrium and at a shear rate of 0.001 fs^{-1} along the three Cartesian planes, xy, xz and yz. For instance, what is shown in figure 6 for the xy plane is the sum of $I_i(\mathbf{q})$ over all possible z values. Notice the nearly circular contour curves in all three planes at equilibrium. Under shear, one finds two crescents appearing

along the meridian in the xy and xz planes, with a circular plot in the yz plane. This signifies nematic ordering in the system [22] and the director is the x axis. If the system showed layering, one would have observed a four-spot pattern, implying smectic ordering. The absence of the four-spot pattern and the presence of crescents confirms the nematic nature of the system under shear. The nematic ordering is observed to relax back to a equilibrium configuration, once the shear stress is relieved.

4. Conclusions

We have studied the effect of planar Couette shear flow on the intermolecular ordering and structure of a room temperature ionic liquid, $[C_{10}mim][PF_6]$. Our simulations reveal interesting changes in the system upon shear. With increasing shear rate, we find a decrease in the magnitude of structural correlations at the nanoscale with a concomitant decrease in the length scale of such correlations as well. The loss in nanoscale order is likely due to decreased structuring at the near-neighbor level of cations and anions. These have been documented using partial pair correlation functions. Interestingly, two partial pair correlation functions, that of tail–anion and head–tail, show an increase in the height of the first peak with increasing shear rate. These can be explained as due to a dilution of specific interactions (charged versus uncharged) at high shear rates. Shear imposes an orientational preference for the cations so as to align their long axes with the shear direction—here the x axis. Apart from demonstrating this preference through orientational distribution functions, contour plots of the structure factor clearly show the emergence of a nematic order in the system, away from equilibrium.

Acknowledgments

References

[1] Wasserscheid P and Welton T (ed) 2003 *Ionic Liquids in Synthesis* (Weinheim: Wiley)
[2] Welton T 1999 *Chem. Rev.* **99** 2071
[3] Rogers R D and Seddon K R 2003 *Science* **302** 792
[4] Gordon C M, Holbrey J D, Kennedy A R and Seddon K R 1998 *J. Mater. Chem.* **8** 2627
[5] De Roche J, Gordon C M, Imrie C T, Ingram M D, Kennedy A R, Celso F L and Triolo A 2003 *Chem. Mater.* **15** 3089
[6] Reichert W M, Holbrey J D, Swatloski R P, Gutowski K E, Visser A E, Nieuwenhuyzen M, Seddon K R and Rogers R D 2007 *Cryst. Growth Des.* **7** 1106
[7] Koddermann T, Paschek D and Ludwig R 2008 *ChemPhysChem* **9** 549
[8] Urahata S M and Rebeiro M C C 2004 *J. Chem. Phys.* **120** 1855
[9] Wang Y and Voth G A 2005 *J. Am. Chem. Soc.* **127** 12192
Wang Y and Voth G A 2006 *J. Phys. Chem.* B **110** 18601
[10] Lopes J N A C and Padua A A H 2006 *J. Phys. Chem.* B **110** 18601
[11] Bhargava B L, Devane R, Klein M L and Balasubramanian S 2007 *Soft Matter* **3** 1395
[12] Bhargava B L, Balasubramanian S and Klein M L 2008 *Chem. Commun.* 3339
[13] Triolo A, Russina O, Bleif H and Cola E D 2007 *J. Phys. Chem.* B **111** 4641
[14] Triolo A, Russina O, Fazio B, Triolo R and Cola E D 2008 *Chem. Phys. Lett.* **457** 362
[15] Heyes D M 1986 *J. Chem. Phys.* **85** 997
Heyes D M 1986 *Chem. Phys. Lett.* **127** 515
[16] Balasubramanian S, Mundy C J and Klein M L 1996 *J. Chem. Phys.* **105** 11190
[17] Yoshio M, Mukai T, Ohno H and Kato T 2004 *J. Am. Chem. Soc.* **126** 994
[18] Evans D J and Morriss G P 1990 *Statistical Mechanics of Nonequilibrium Liquids* (London: Academic)
[19] Plimpton S J 1995 *J. Comput. Phys.* **117** 1 Version: 5 October 2007
[20] Hoover W G 1985 *Phys. Rev.* A **31** 1695
[21] Bates M A and Luckhurst G R 2003 *J. Chem. Phys.* **118** 6605
[22] de Vries A 1973 *Liquid Crystals: Proc. Int. Conf.* ed S Chandrasekhar; *Pramana Suppl.* **1**, p 93